DYNAMIC AND STATIC STRUCTURAL ANALYSIS OF LIQUID LITHIUM BLANKET OF FUSION POWER PLANT

M. MASUDA, T. HORIE, G. YAGAWA, Y. ANDO

Department of Nuclear Engineering, University of Tokyo,
3-1 Hongo, 7-Chome, Bunkyo-ku, Tokyo 113, Japan

SUMMARY

In several conceptual designs of Tokamak type fusion reactors, liquid lithium is used as the coolant of the blanket together with the purpose of tritium breeding. In such designs, magnetohydrodynamic (MHD) effect is one of the most important problems for the blanket structure because of the high electrical conductivity of liquid lithium.

The purpose of this paper is to make clear some of the structural problems concerning the design of liquid lithium blanket of fusion reactor. In this connection, taking UWMAK-III design which was developed at University of Wisconsin, we analyze not only the structural but also thermo-fluid behaviors of liquid lithium blanket.

In terms of the nondimensional numbers, i. e. magnetic Reynolds number, Hartmann number and magnetic interaction number, we simplify the basic equations of MHD flows. Then, we solve the pressure, velocity and temperature fields in the blanket with these equations. The results of these calculations are used as inputs for the static as well as dynamic analyses of the structural behaviors of the blanket where we use straight beam elements in approximating the geometry of the blanket and the calculation is based upon the elastoplastic large deflection theory.

It is found from the static analysis that the local bending moments are most significant near the connections of cylindrical and flat parts of the first wall. As the dynamic response of liquid lithium blanket, we assume such an accident of the reactor that the plasma current is cut off in very short time. In this case, we take account of the compressibility of liquid lithium because the phenomenon should be considered as a kind of shock caused by electromagnetic force. It is found from the result of calculations that the pressure in the blanket rises considerably near the top of the first wall, and that the peak value of the pressure depends on the intensity of the toroidal magnetic field. It is also found from the structural analysis based on the above flow analysis that more of the half thickness has yielded on the top of the first wall.

Finally, the crack analysis including the dynamic electromagnetic body force effect is performed. This analysis is based upon the linear fracture mechanics and the dynamic stress intensity factor is estimated by the 2-dimensional finite element code with distorted 8 nodes isoparametric elements. The phenomenon is considered to be one of the important problems from the viewpoint of safety of the fusion power plants.

1. INTRODUCTION

Several conceptual designs of Tokamak fusion reactors have been published in order to study the engineering problems that will be faced in the actual design [1]-[3]. It has been pointed out there that the large pressure drop due to magnetohydrodynamic (MHD) effect is a serious problem when liquid lithium is used as the coolant for the blanket. Futhermore, the MHD effect will have influence on the thermal and mechanical behaviors of liquid lithium blanket. Therefore, the thermal, fluid and mechanical behaviors of liquid lithium blanket must be analyzed all together.

The purpose of this paper is to make clear some of the coupled problems of liquid lithium blanket. We have already reported the static analysis of this coupled problem in Ref. [4]. Therefore, in this paper we are mainly concerned with the dynamic analysis of liquid lithium blanket. In addition, the dynamic fracture problem caused by the dynamic electromagnetic force is analyzed based upon the linear fracture mechanics, because the phenomenon is considered to be one of the important problems from the viewpoint of safety of the fusion plants.

[NOMENCLATURE]

$\vec{B}$: magnetic induction. $\vec{E}$: electric field. E: Young's modulus. H: work hardening coefficient. $\vec{J}$: electric current vector. K_I: stress intensity factor. K_{Ic}: fracture toughness. p: pressure. u and v: x and y components of $\vec{V}$, respectively. $\vec{V}$: velocity vector. V_s: sonic velocity. α: linear expansion coefficient. ν: Poisson's ratio. ρ: mass density. σ_e: electrical conductivity. σ_y: yield stress. $( )^*$: deviation from steady state. $( )_\alpha$: nodal value. $( )_i$: component in the coordinate i. $( )_{,i}$: partial differentiation with respect to the coordinate i. $\dot{( )}$: partial differentiation with respect to time. $\vec{\nabla}$: $(\frac{\partial}{\partial x}, \frac{\partial}{\partial y}, \frac{\partial}{\partial z})^T$

2. ANALYSIS OF FIRST WALL

Here, we discuss briefly the outer blanket of UWMAK-III design which was developed at University of Wisconsin [3]. The detail of the outer blanket is shown in Fig. 1 which is the cross sectional view in the toroidal direction. The cell of heat transfer unit is a U-shaped channel which has 10cm wide static zone in the middle. One of the U-shaped channels which we are concerned with is idealized as shown in Fig. 2. We assume that the problem is 2-dimensional in the x-y plane and that the uniform steady magnetic induction B_z and non-uniform unsteady magnetic induction B_y are applied to the whole region, which correspond to the toroidal and poloidal fields, respectively.

Next, we simplify the MHD equations using the nondimensional numbers. The Hartmann number H_a is set to be 10^5 in UWMAK-III design. From this condition, we may ignore the viscous force compared with the magnetic force. The average fluid velocity is around 1.0cm/sec, then the Reynolds number R_e is approximately 10^3. On the other hand, the magnetic Prandtl number P_{rm} of liquid lithium is about 10^{-6}. From these informations, the magnetic Reynolds number R_m can be calculated to be $R_m = P_{rm} \cdot R_e \approx 10^{-3}$. This allows us to neglect the induced magnetic field compared with the applied magnetic field. The magnetic interaction number N can be calculated from the Hartmann and Reynolds numbers to be $N = H_a^2/R_e \approx 10^7$. This condition implies that we may ignore the inertia force compared with the magnetic force.

Applying the above informations to the Navier-Stokes equation, we obtain the following equation.

$$\rho\dot{\vec{V}} + \vec{\nabla}p - \vec{J} \times \vec{B} = 0 \tag{1}$$

The equation of continuity in the 2-dimensional form can be written as follows.

$$\dot{\rho} + (\rho u)_{,x} + (\rho v)_{,y} = 0 \tag{2}$$

The relation between the electric current density and the velocity fields is given by the Ohm's law as

$$\vec{J} = \sigma_e(\vec{E} + \vec{V} \times \vec{B}) \tag{3}$$

Substitution of eq. (3) into eq. (1) yields the following 2-dimensional equations.

$$\rho\dot{u} + p_{,x} - \sigma_e E_y B_z + \sigma_e(B_y^2 + B_z^2)u + \sigma_e E_z B_y = 0 \tag{4a}$$

$$\rho\dot{v} + p_{,y} + \sigma_e E_x B_z + \sigma_e B_z^2 v = 0 \tag{4b}$$

In the dynamic analysis, we take account of the compressibility of liquid lithium. Then, the constitutive equation between the pressure and the mass density is needed in addition to eqs. (2) and (4). That is

$$p^*/\rho^* = V_e^2 \tag{5}$$

The finite element equations of eqs. (2) and (4) can be written as follows.

$$[\Pi_{\alpha\beta}]\begin{Bmatrix} \dot{\rho}^*_\beta \\ \dot{u}^*_\beta \\ \dot{v}^*_\beta \end{Bmatrix} + [\Lambda_{\alpha\beta}]\begin{Bmatrix} \rho^*_\beta \\ u^*_\beta \\ v^*_\beta \\ p^*_\beta \end{Bmatrix} + \Gamma_\alpha = 0 \tag{6}$$

where it is noted that the discretized variables are the deviations from the steady state. These equations are solved with the explicit finite-difference time-marching scheme.

In the structural analysis of the blanket, we use the straight beam elements in approximating the geometry of the blanket, first wall and baffles. The finite element equation including the dynamic effect can be derived from the principle of virtual work as follows.

$$M_{\alpha\beta}\Delta\ddot{\omega}_\beta + (K^e_{\alpha\beta} + K^g_{\alpha\beta} + K^p_{\alpha\beta})\Delta\omega_\beta = \Delta F_\alpha \tag{7}$$

where $M_{\alpha\beta}$ is the mass matrix, and $K^e_{\alpha\beta}$, $K^g_{\alpha\beta}$ and $K^p_{\alpha\beta}$ are the stiffness matrices representing the linear elastic, geometrical nonlinear and plastic behaviors, respectively. In addition, ΔF_α and $\Delta\omega_\alpha$ are the incremental load and displacement vectors, respectively. The above equation is solved step by step with Newmark's β method (β=1/4).

2.1. STATIC ANALYSIS OF FIRST WALL

The first wall is made from the molybdenum alloy TZM in the UWMAK-III design and the following material properties are assumed in the analysis.

$$E=2.8\times10^4 kg/mm^2, \quad \sigma_y=20kg/mm^2, \quad H=E/1000, \quad \alpha=5.5\times10^{-6}1/K, \quad \rho=10.2g/cm^3$$

Figure 3 shows the calculated skin stresses of outer and inner surfaces of the first wall. It can be seen from this figure that there is notable difference between the results based upon the linear elastic and large deflection elastoplastic theories. In this figure, the small deflection theory gives the unacceptable result. On the other hand, the result of nonlinear analysis shows the moderate stress distribution except the local bending stress observed at points B and D due to the geometrical gross discontinuity. It can be also seen that the signs of the moments at points B and D are opposite to each other. This will be due to the fact that the load acts on the first wall roughly in (-y) direction, which is caused

by the large MHD pressure drop in the channel. The points B and D are welded or brazed for the connection of cylindrical and flat parts of the first wall. Therefore, it may be considered from the design point of view that we should pay our attention to this kind of parts in the first wall structure.

2.2. DYNAMIC ANALYSIS OF FIRST WALL

Here, we assume such an accident of reactor that the plasma current is cut off in very short time as shown in Fig. 4. Because the phenomenon is considered as a kind of shock caused by electromagnetic force, we take account of the compressibility of liquid lithium. The induced electric current J_z and the poloidal magnetic induction B_y in lithium zone are calculated by the finite element code [5].

The time variation of dynamic MHD pressure at point C (see Fig. 2) is shown in Fig. 5. It can be seen from this figure that the peak value of the dynamic MHD pressure depends upon the intensity of the toroidal field. This result is consistent with the fact that the magnetic field acts as the damping force in the wave propagation in the fluid. In Fig. 6, we show the time variation of the pressure distribution along the inner surface of the first wall, where t_p and B_z are set to be 25μsec and 4.05Wb/m^2, respectively. It can be seen from this figure that the maximum value of the dynamic pressure is observed at the top of the first wall (point C), and it becomes about two times larger than the static one. This result is used as the input for the following structural analysis. Figure 7 depicts the skin stresses of outer and inner surfaces along the first wall. It can be seen from this figure that the large bending moment is significant along the first wall and the profile of the stresses is consistent with the dynamic MHD pressure distribution shown in Fig. 6. Figure 8 shows the distributions of stress in the thickness direction at the top of the first wall. In Fig. 9, we show the yielded region in the first wall at time 70μsec after the plasma current begins to drop. It can be seen from these two figures that more than half thickness has yielded at the top of the first wall by 70μsec.

3. PRELIMINARY ANALYSIS OF CRACK UNDER ELECTROMAGNETIC BODY FORCE

We have a plan of an elementary experiment concerning the fracture caused by the dynamic electromagnetic body force. The schematic view of the experiment is shown in Fig. 10. In this figure, the uniform and static magnetic induction B_0 is applied in z direction, and the dynamic electric current I_x is given in x direction. Thus, the beam with crack may deform in (-y) direction by means of the Lorenz force, i. e. the opening mode for the crack will be observed.

In this paper, we show only the result of K_I estimation prior to the experiment. Stress intensity factor K_I is estimated by the 2-dimensional finite element code with the distorted 8 nodes isoparametric elements [6,7]. The finite element equation for the problem can be written formally as follows.

$$M_{\alpha\beta}\ddot{\omega}_\beta + K_{\alpha\beta}\omega_\beta = F_\alpha \qquad (8)$$

where $M_{\alpha\beta}$, $K_{\alpha\beta}$, ω_α and F_α are the mass matrix, stiffness matrix, displacement vector and load vector, respectively.

The dynamic electric current I_x is assumed as shown in Fig. 11 and the magnetic induction B_0 is set to be 0.8Wb/m^2. The material of the test specimen is an aluminum alloy

and the following material properties are assumed in the calculation.

$$E=10^{4}\,kg/mm^{2},\quad \rho=2.7\,g/cm^{3},\quad \nu=0.3$$

Figure 12 shows the calculated K_I value. It can be seen from this figure that the rate of stress intensity factor $\dot{K}_I$ almost reaches $10^{5}\,kg/(mm^{3/2}\cdot sec)$. Therefore, it may be important to take into account the dynamic effect on the material property K_{Ic} in the actual experiment.

[ACKNOWLEDGEMENT]

The authors gratefully acknowledge kind advices of the members of steering committee of basic experimental facility for blanket of nuclear fusion reactor, the faculty of engineering, University of Tokyo.

[REFERENCES]

[1] A. P. FRAAS, "Conceptual Design of the Blanket and Shield Region and Related Systems for a Full Scale Toroidal Fusion Reactor", ORNL-TM-3096, Oak Ridge National Laboratory (1973).

[2] R. G. MILLS, "A Fusion Power Plant", MATT-1050, Princeton Plasma Physics Laboratory (1974).

[3] B. BADGER, et al., "A Noncircular Tokamak Power Reactor Design, UWMAK-III", UWFDM-150, University of Wisconsin (1976).

[4] G. YAGAWA, et al., "Finite Element Analysis of Magnetohydrodynamics and its Application to Lithium Blanket Design of Fusion Reactor", Presented at U. S. - JAPAN SEMINAR on Interdisciplinary Finite Element Analysis, Ithaca, New York, U. S. A. (1978).

[5] K. MIYA, et al., "Application of Finite Element Method to Electro-magneto-mechanical Dynamics of Superconducting Magnet Coil and Vacuum Vessel", Proc. of 6-th Symposium on Engineering Problems of Fusion Research, San Diego, California, U. S. A., pp. 927-934 (1975).

[6] R. D. HENSHELL and K. G. SHAW, "Crack Tip Finite Elements are Unnecessary", Int. J. Num. Meth. Engng., Vol. 9, pp. 495-507 (1975).

[7] R. S. BARSOUM, "On the Use of Isoparametric Finite Elements in Linear Fracture Mechanics", Int. J. Num. Meth. Engng., Vol. 10, pp. 25-37 (1976).

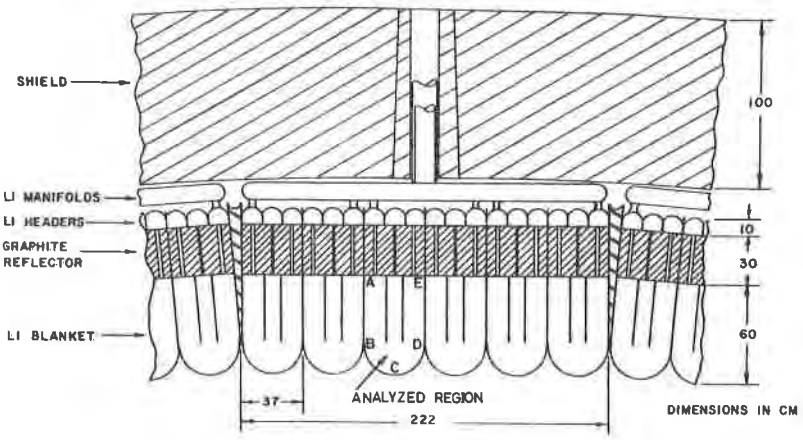

Fig. 1 cross sectional view of the outer blanket in UWMAK-III design (cited from Ref. [3]).

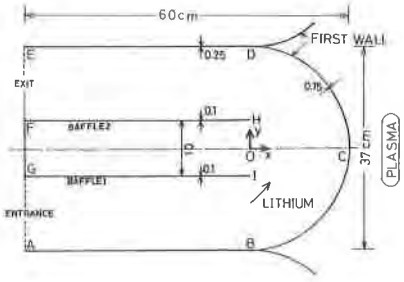

Fig. 2 idealization for a U-shaped channel.

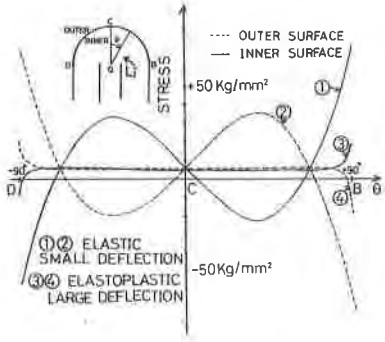

Fig. 3 distributions of skin stresses of inner and outer surface of the first wall.

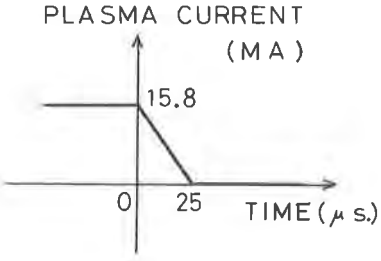

Fig. 4 assumed time dependence of plasma current.

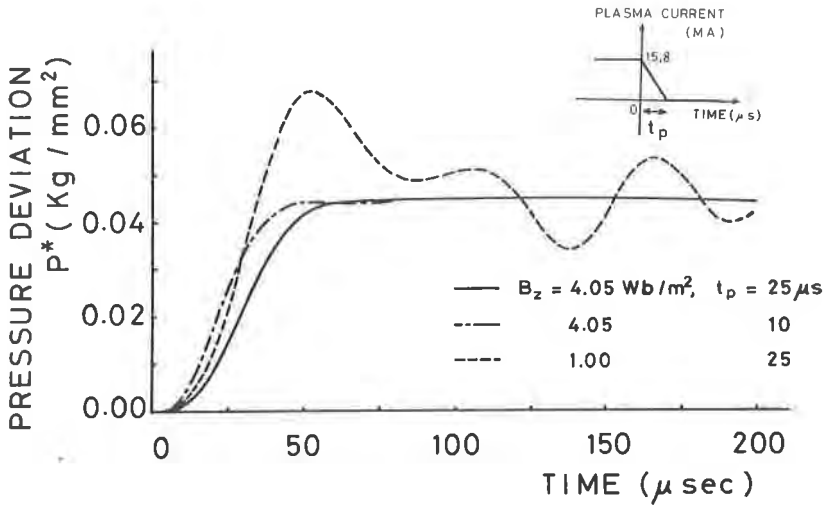

Fig. 5 time variation of pressure at the top of the first wall.

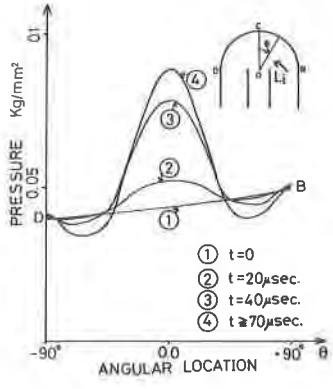

Fig. 6
time variation of pressure distribution along the inner surface of the first wall.

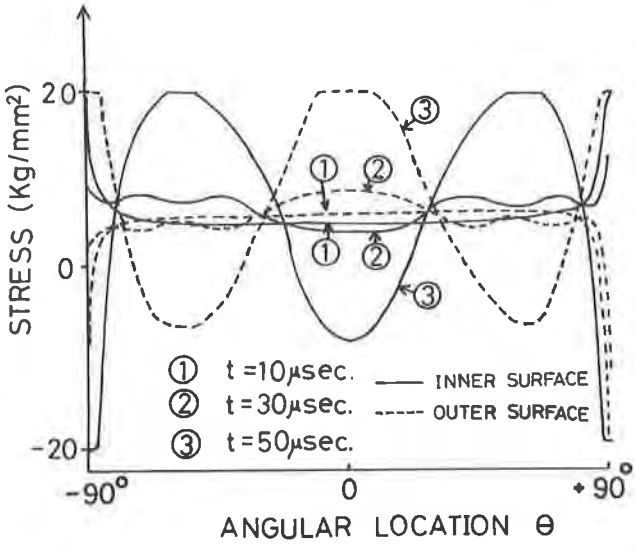

Fig. 7 distributions of skin stresses of inner and outer surfaces of the first wall.

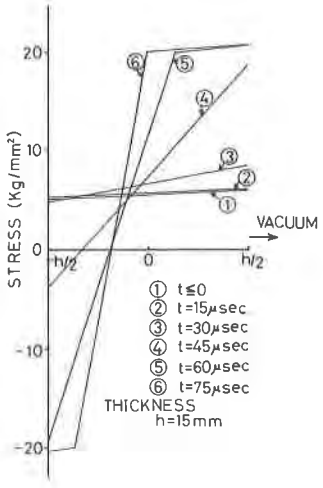

Fig. 8
stress distributions in the thickness direction at the top of the first wall.

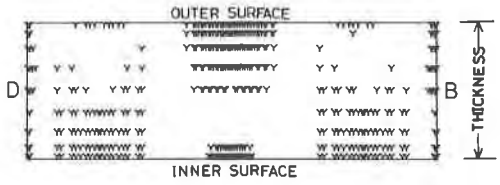

Fig. 9 yielded region in the first wall at time 70μsec.

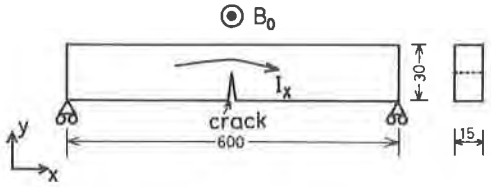

Fig. 10 the geometry of the dynamic crack analysis.

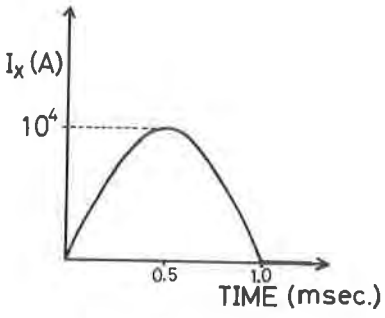

Fig. 11 assumed current I_x with time.

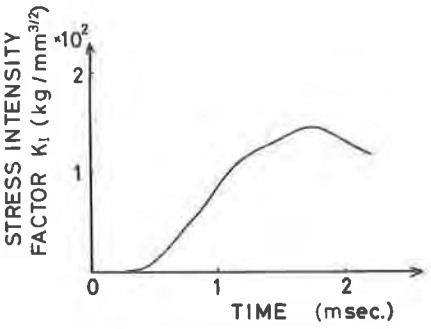

Fig. 12 calculated time variation of stress intensity factor K_I.